



ELSEVIER

Journal of Non-Crystalline Solids 293–295 (2001) 112–117

JOURNAL OF
NON-CRYSTALLINE SOLIDS

www.elsevier.com/locate/jnoncrsol

EXAFS studies of the local structure of Er³⁺ ions in silica xerogels co-doped with aluminium

F. Rocca^{a,*}, M. Ferrari^a, A. Kuzmin^b, N. Daldosso^c, C. Duverger^c, F. Monti^d^a *CeFSA – Centro CNR-ITC di Fisica degli Stati Aggregati, Via Sommarive 18, 38050 Povo (Trento), Italy*^b *Institute of Solid State Physics, University of Latvia, Kengaraga street 8, LV-1063 Riga, Latvia*^c *INFM and Dipartimento di Fisica, Università di Trento, Via Sommarive 14, 38050 Povo (Trento), Italy*^d *Dipartimento Scientifico e Tecnologico, Università di Verona, Strada Le Grazie, 37134 Verona, Italy*

Abstract

The local environment around Er³⁺ ions in wet and densified (at 900°C) silica xerogels (pure and co-doped with aluminium) has been studied at the Er L₃-edge by X-ray absorption spectroscopy using the fluorescence detection technique. The radial distribution functions (RDF), reconstructed from X-ray absorption fine structure (EXAFS), show several changes in the local co-ordination of erbium ions upon densification: shortening of the Er–O and Er–Si/Al distances, decrease of the co-ordination numbers and broadening of the Er–O RDF. The effect of Al co-doping is clearly discerned by EXAFS in both the first and second co-ordination shells for densified gels and mainly in the second shell for wet gels. For increasing Al content, the interatomic distances between erbium ions and the second co-ordination shell ions become longer and have narrower distribution. A preferential bonding of Er to Al ions is clearly detected, with increasing ordering at higher Al content. EXAFS does not show evidence of a clustering for Er³⁺ ions after densification: the short range Er–Er co-ordination is absent or not detectable in the present experiments. © 2001 Elsevier Science B.V. All rights reserved.

1. Introduction

There is great interest in research directed to the development of erbium-doped silica-based glasses obtained by the sol–gel route [1,2]. Silica-based sol-gel glasses activated by Er³⁺ ions are attractive materials for integrated optics devices such as frequency up converters and optical amplifiers operating in the 1.5 μm band [1,2]. The main determinants of the performance of sol–gel-based devices are the non-radiative relaxation channels

due to rare-earth (RE) concentration quenching and vibrations of the OH groups. In integrated Er amplifiers, few centimeters of optical path are needed, and the erbium concentration should be as high as possible to obtain good optical amplification gain [1]. However, at increasing Er concentration, non-radiative energy transfer between neighbouring ions (attributed to clustering of the RE ions) may take place and lead to both linear and non-linear quenching [2]. Earlier spectroscopic studies have shown that the concentration and the properties of the optically active ion affect the densification and the optical properties of the final glass [2–5]. Alumina addition was found to improve the dispersion of the optically active ion in silica glasses prepared by sol-gel route [1,4,6].

* Corresponding author. Tel.: +39-0461 881 685; fax: +39-0461 881 680.

E-mail address: rocca@science.unitn.it (F. Rocca).

In order to optimize the performance of the RE ions-doped glasses, detailed structural information in particular on the local structure of the optically active ion is required [7–12]. The local structure around the RE ions can be investigated by several techniques such as luminescence spectroscopy [13,14], X-ray absorption fine structure (EXAFS) [8,15,16] and molecular dynamics simulation [12].

Recently some of us presented an EXAFS study of Pr^{3+} [9] and Tb^{3+} [10] doped silica xerogels as a function of the heat treatment and the RE content. The measurements have shown that densification induces a decreasing of the co-ordination number and a shortening of the main RE–O distance. Moreover no evidence of ordered RE–RE correlation was found.

In the present work, we extend our previous studies [9,10] reporting on a X-ray absorption spectroscopy study of the local environment around Er^{3+} ions in silica xerogels co-doped with aluminium. The influence of the Al concentration on the short range structure around Er^{3+} ions is discussed.

2. Experimental and data analysis

A series of transparent, monolithic silica xerogels with different Er/Al molar ratios (1:0, 1:6, 1:9) was prepared using the procedures described in our previous papers [4,9]. The erbium concentration was in the range from 400 to 10 000 ppm: in the following we will present only the 2000 ppm samples. After preparation, the wet xerogels were stored in a muffle furnace at about 60°C for 5 days, and slowly cooled afterwards to room temperature. Thus obtained glasses were transparent/opaque and monolithic. We will refer to them as wet non-treated (NT) xerogels. Some samples were further densified at 900°C during 120 h with a heating rate of 0.1°C/min: these will be referred as high-temperature (HT) treated xerogels.

The reference compounds, used in the EXAFS data analysis, were polycrystalline Er_2O_3 , ErVO_4 and $\text{Er}(\text{OH})_9(\text{CF}_3\text{SO}_3)_3$, and 0.1 M aqueous solution of $\text{Er}(\text{NO}_3)_3 \cdot 5\text{H}_2\text{O}$ salt.

X-ray absorption spectra (XAS) of silica xerogels were recorded at the Er L_3 -edge in fluores-

cence mode at ESRF (Grenoble, France) on the BM8 GILDA CRG beamline.

XAS were treated by the EDA software package [17–20] using a similar approach as in our previous works on praseodymium- and terbium-doped silica xerogels. The position of the photoelectron energy origin E_0 , utilised in the calculation of the EXAFS wave vector k , was set at the white line maximum. The experimental EXAFS signals $\chi(k)k^2$ were extracted using the usual procedure [17,18], and the contributions from the first and second co-ordination shells were singled out by the Fourier filtering technique. The Fourier transforms (FTs) for 2000 ppm Er-doped xerogels are shown in Fig. 1.

Structural parameters were obtained by a conventional multi-shell Gaussian best fit of the EXAFS signals, singled out by the back-FT procedure in the range from 0.8 to 3.8–4.0 Å. These EXAFS signals contain two contributions: from the first shell (the peak at 1.8 Å), composed of oxygen atoms, and from the second shell (the peak at 2.8–3.5 Å), composed of oxygen and silicon/aluminium atoms. Note that, as first step of analysis, we have neglected the multiple-scattering (MS) effects within the first and second shells (which, in principle, may influence the results for the second shell), because our estimates for several erbium–oxygen clusters, based on the FEFF6 calculations [21,22], suggest that the MS contribution should be small compared to the single-scattering signals. Additionally, the second shell peak at 2.8–3.5 Å (Fig. 1) exhibits a clear dependence on the concentration of aluminium ions that supports their dominant contribution in the second shell. In any case, due to the weakness of the second shell EXAFS signal, the short range interval ($k = 1.5\text{--}8.2 \text{ \AA}^{-1}$) utilised for the data analysis and the relatively noisy signal, we did not search for precise information on the second shell structure. Our main goals were to determine the type of atoms, located in the second shell, and to estimate the interatomic distances, whereas the accurate determination of the co-ordination numbers and the broadening factors (the Debye–Waller terms) was left out. A more extensive analysis on the whole set of measured samples is in progress.

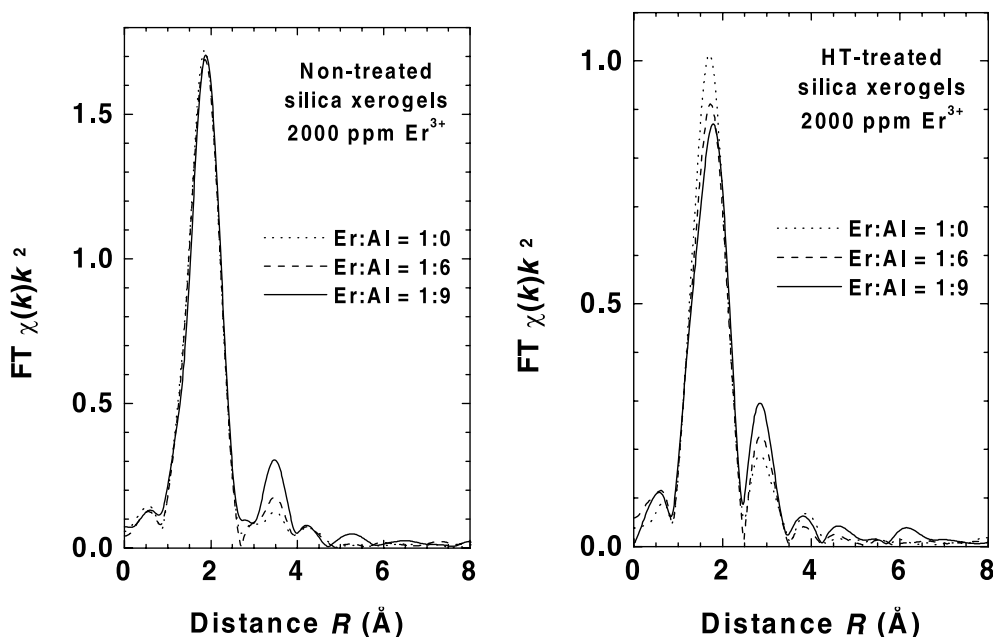


Fig. 1. Fourier transforms of the experimental Er L_3 -edge EXAFS signals $\chi(k)k^2$.

To perform the modeling of the EXAFS spectra, one needs to know the scattering amplitude and phase shift functions for each atom participating in the scattering process. These data for the nearest oxygen atoms were extracted within the Gaussian approximation from the experimental EXAFS signal of the erbium nitrate aqueous solution [23], assuming the following structural parameters for hydrated erbium ion [24]: the coordination number $N = 8$, the interatomic distance $R(\text{Er-O}) = 2.36 \text{ \AA}$, the Debye–Waller factor $\sigma^2 = 0.007 \text{ \AA}^2$. Since in the xerogels the first shell makes the dominant contribution to the EXAFS signals, we were especially interested to check the reliability of the Er–O scattering functions. They were used to best fit the first shell EXAFS signals of the reference compounds, and the obtained structural parameters were compared with known values from X-ray or neutron diffraction: good agreement was found for the interatomic distances in all cases.

For the second shell co-ordination, following the same procedure previously performed for terbium-doped xerogels [10], theoretical data for Er–O, Er–V and Er–Er atom pairs were calculated by

the FEFF6 code [21,22] and optimised to reproduce the experimental EXAFS of the $c\text{-ErVO}_4$. Er–Si and Er–Al theoretical signals were then calculated by substituting Al and Si to V in the $c\text{-ErVO}_4$ structure. Thus, the scattering amplitude and phase shift functions were obtained for all the interesting atom pairs.

3. Results

The FTs of the EXAFS signals (Fig. 1) indicate the amorphous nature of the local environment around erbium ions in silica xerogels. In fact, only two nearest co-ordination shells, located below 4 Å, produce well-defined peaks in FTs (with the first shell being dominant), whereas the outer shells contributions are smeared out by disorder. The behaviour of the peak at 1.8 Å, corresponding to the first shell, is, in general, similar to that found by us previously in praseodymium and terbium xerogels [9,10]: the peak broadens and shifts to shorter distances upon HT treatment, but does not show significant dependence on the RE dopant concentration. However, both the first and second

shell peaks are sensitive to the co-doping with aluminium ions, especially after heat treatment. By going from xerogel without aluminium (Er:Al = 1:0) to the one with the highest aluminium content (Er:Al = 1:9), the first peak amplitude decreases in densified xerogels but is nearly unchanged in the wet xerogels. At the same time, the second peak amplitude increases in both cases.

In Fig. 2 we present the RDFs, obtained by the conventional multi-shell Gaussian approach, for 2000 ppm Er³⁺-doped silica xerogels with different aluminium content. The first shell in NT xerogels is composed of about 7–8 oxygen atoms, located at 2.40 ± 0.02 Å. Upon HT treatment, the number of oxygens in the first shell decreases by one atom to about 6–7, and the average Er–O distance shortens from 2.40 to 2.32 Å in xerogels without aluminium and from 2.40 to 2.37 Å in xerogels co-doped with aluminium. Besides, we can observe a strong increase of the first shell broadening: the Debye–Waller factor σ^2 increases from 0.007 to $0.02\text{--}0.04$ Å².

The second shell peak is mainly due to a co-ordination of Er with silicon and aluminium at-

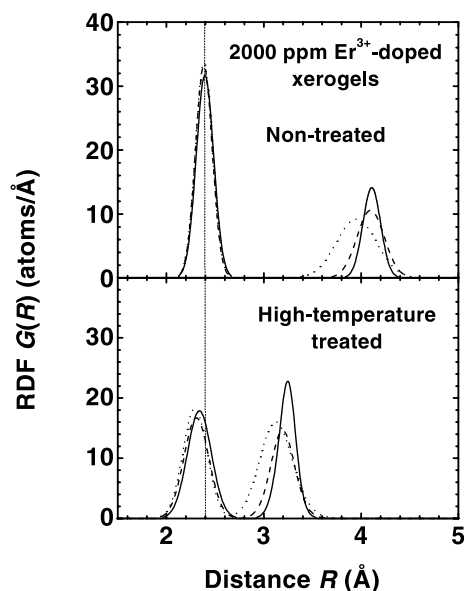


Fig. 2. Radial distribution functions $G(R)$ around Er³⁺ ions in NT and HT treated (at 900°C) silica xerogels. Without Al: dotted line; co-doped with Al: dashed line (Er:Al = 1:6); solid line (Er:Al = 1:9).

oms. EXAFS analysis excludes a direct Er–Er co-ordination at this distance. Some contribution from oxygen atoms cannot be also excluded, however its precise determination is beyond our accuracy. As one can see in Fig. 2, the second shell peak experiences dramatic change upon densification: the average interatomic distances shorten from ~ 4.0 Å in NT xerogels to 3.14 Å for densified gels without Al and to 3.22 Å for Er:Al = 1:9. The co-doping with aluminium results in lower contraction, and smaller broadening. The latter fact is the main reason for an increase of the second shell peak amplitude at 3–3.5 Å in Fig. 1 for higher aluminium content. In fact, the Er–Si/Al co-ordination number is 4–5 for NT xerogels and 3–4 for the densified ones: its dependence on co-doping with Al is negligible, remaining within the uncertainty of analysis, which was evaluated to be ± 0.7 atoms by comparison of repeated experiments and different data analysis procedures.

4. Discussion

At first, we observe that the structural information on the local surrounding of Er ions in silica xerogels is in good agreement with our previous results for Pr and Tb ions obtained using X-ray absorption spectroscopy [9,10].

For the first co-ordination shell around RE (Er, Tb, Pr) ions in silica xerogels, a general tendency upon thermal treatment is observed and can be described as: a decrease of the total co-ordination number, an asymmetric broadening of RDF, a shortening of the average RE–oxygen bonds length. The observed significant differences between the average interatomic distances for the three RE ions follow the difference of their ionic radii [25]. We may also note that the asymmetry of the first shell in Er-doped xerogels is smaller than in Tb- or Pr-doped xerogels. This is probably due to the stronger Er–O bonding caused by a higher degree of electro-positivity of erbium ions.

Further, we will discuss the variations occurring upon densification within the second co-ordination shell. As was stated previously, due to the very weak second shell contribution and the relatively low signal-to-noise ratio of the fluorescence sig-

nals, the most reliable information on the second shell is related to the interatomic distances.

It is necessary to point out also that since silicon and aluminium atoms are neighbours in the periodic table, it is a bit tricky to distinguish between them in the EXAFS spectra. However, the observed variation of the second shell peak intensity with the concentration of aluminium (Fig. 1) allows us to suppose that in aluminium co-doped xerogels, aluminium atoms enter the second co-ordination shell of erbium. This hypothesis is supported by the changes in both first and second shell distances. In particular, we remember here that the second peak position increases by about 0.08 Å going from undoped (Er:Al=0) to co-doped (Er:Al=1:9) xerogels. Such behaviour can be explained by the longer value of the Al–O distances ($R(\text{Al–O})=1.76$ Å in tetrahedral co-ordination and $R(\text{Al–O})=1.94$ Å in octahedral co-ordination) compared to the typical Si–O distances ($R(\text{Si–O})=1.62$ Å). These results suggest that aluminium ions are located in the neighbourhood of erbium and agree with the known fact that aluminium ions are mainly distributed within the pores of silica gel, where the RE ions enter.

Finally, we can estimate the variation of the Er– $\hat{\text{O}}$ –Si/Al angles after the full densification of xerogels. Taking the values of the Er–O and Er–Si/Al distances measured by EXAFS, one finds that the average Er– $\hat{\text{O}}$ –Si/Al angles vary significantly upon HT treatment. We assume that silicon ions, forming the xerogel network, are tetrahedrally coordinated, whereas aluminium ions may have either tetrahedral or octahedral co-ordination (when they participate in the xerogel network formation or are located at the surface of the xerogel pores, respectively) [26]. This kind of bonding was suggested in aluminosilicate glasses doped by Eu^{3+} [27], where a linkage of europium ions to both AlO_4 and AlO_6 structural units was found.

The estimated changes are: for Er– $\hat{\text{O}}$ –Si from 162° to $\sim 105^\circ$; for Er– $\hat{\text{O}}$ –Al from 164° to 101° for tetrahedrally co-ordinated and from 143° to 96° for octahedrally co-ordinated aluminium ions.

In these NT xerogels, the Er– $\hat{\text{O}}$ –Si/Al bond angles correspond to the vertex shared connection between erbium and silicon/aluminium polyhedra. Upon densification, the shortening of the Er–O

and Er–Si/Al distances leads to a decrease of the bond angle values by about 50° . This implies that the bond angle values, in case of a corner sharing connection of erbium–oxygen polyhedra to the SiO_4 or AlO_4 tetrahedra, become significantly less than the usual Si– $\hat{\text{O}}$ –Si bond angle (144°) in silica glass. The second possible type of bonding is related to the connection of erbium and aluminium oxygen polyhedra through the edges. It corresponds to a smaller value for the Er– $\hat{\text{O}}$ –Al angle. This arrangement has been found, for example, in crystalline $(\text{Er}_x\text{Y}_{1-x})_3\text{Al}_5\text{O}_{12}$ garnet solid solutions [28].

The observation of an increasing order at higher Al-content (lower Debye–Waller factor) could suggest that the more probable connection is the edge-sharing connection of erbium–oxygen polyhedra to AlO_6 octahedra. However, from the present EXAFS data it is impossible to discriminate with certainty between the two possible Al-co-ordinations.

5. Conclusions

The local atomic structure around Er^{3+} ions has been studied by X-ray absorption spectroscopy in 2000 ppm Er-doped and Er/Al-co-doped silica xerogels, with Er/Al molar ratio set to 1:0, 1:6 and 1:9. Both wet and densified xerogels were studied. Similarly to Pr- and Tb-doped silica xerogels [9,10], the local structure around Er is strongly changed upon densification: in the first shell, the shortening of the Er–O distances is accompanied by a decrease of the co-ordination number and by a broadening of the RDF. The contraction of the interatomic distances upon densification was also found in the second co-ordination shell, which is attributed to silicon/aluminium atoms. The presence of Er–Er co-ordination shell is not detected by EXAFS, which is, on the contrary, quite sensitive to the effects of Al co-doping. At increasing Al content, the second shell distance becomes slightly longer, and the radial distribution becomes narrower, due to lower Debye–Waller factor, indicating a progressive ordering of Si/Al atoms.

These results suggest that aluminium ions are located in the neighbourhood of erbium in both

wet and densified xerogels: they are mainly distributed within the pores of silica gel, where the RE ions enter. The preferential substitution of Si by Al atoms in the local environment of erbium is at the origin of the improvement of optical properties shown by Al co-doped silica gels.

Acknowledgements

Authors would like to thank Mrs C. Armellini for the preparation and characterisation of xerogel samples and Dr G. Pucker for fruitful discussions. A. Kuzmin wish to thank the Centro CNR-ITC di Fisica degli Stati Aggregati (Trento) and the Università di Trento for hospitality and financial support. The financial support by ESRF (project HS612-1998) is acknowledged. Authors are grateful to the staff of the BM8-GILDA beamline for assistance during the measurements.

References

- [1] X. Orignac, D. Barbier, X.M. Du, R.M. Almeida, O. McCarthy, E. Yeatman, *Opt. Mater.* 12 (1999) 1.
- [2] B.T. Stone, K.L. Bray, *J. Non-Cryst. Solids* 197 (1996) 136.
- [3] C. Armellini, L. Del Longo, M. Ferrari, M. Montagna, G. Pucker, P. Sagoo, *J. Sol-Gel Sci. Technol.* 13 (1998) 599.
- [4] C. Armellini, M. Ferrari, M. Montagna, G. Pucker, C. Bernard, A. Monteil, *J. Non-Cryst. Solids* 245 (1999) 115.
- [5] C. Duverger, M. Montagna, R. Rolli, S. Ronchin, L. Zampedri, M. Fossi, S. Pelli, G.C. Righini, A. Monteil, C. Armellini, M. Ferrari, *J. Non-Cryst. Solids* 280 (2001) 261.
- [6] M. Nogami, Y. Abe, *J. Non-Cryst. Solids* 197 (1996) 73.
- [7] J. Wang, W.S. Brocklesby, J.R. Lincoln, J.E. Townsend, D.N. Payne, *J. Non-Cryst. Solids* 163 (1993) 261.
- [8] R.M. Almeida, H.C. Vasconcelos, M.C. Gonçalves, L. Santos, J. Non-Cryst. Solids 232 (1998) 65.
- [9] F. Rocca, G. Dalba, R. Grisenti, M. Bettinelli, F. Monti, A. Kuzmin, *J. Non-Cryst. Solids* 232–234 (1998) 581.
- [10] F. Rocca, F. Monti, A. Kuzmin, A. Dalmaso, D. Pasqualini, *J. Synchrotron Rad.* 6 (1999) 737.
- [11] X. Orignac, H.C. Vasconcelos, R.M. Almeida, *J. Non-Cryst. Solids* 217 (1997) 155.
- [12] S. Chausseidant, C. Bernard, A. Monteil, N. Balu, J. Obriot, S. Ronchin, C. Tosello, M. Ferrari, *SPIE* 3942 (2000) 243.
- [13] R. Campostrini, G. Carturan, M. Ferrari, M. Montagna, O. Pilla, *J. Mater. Res.* 7 (1992) 745.
- [14] D. Levy, R. Reisfeld, D. Avnir, *Chem. Phys. Lett.* 109 (1984) 593.
- [15] L.D. Carlos, R.A. Sá Ferreira, V. De Zéa Bermudez, C. Molina, L.A. Bueno, S.J.L. Ribeiro, *Phys. Rev. B* 60 (1999) 10042.
- [16] A. Terrasi, G. Franzò, S. Coffa, F. Priolo, F. d'Acapito, S. Mobilio, *Appl. Phys. Lett.* 70 (1997) 1712.
- [17] A. Kuzmin, *Physica B* 208&209 (1995) 175.
- [18] A. Kuzmin, *J. Phys. IV (Fr.)* 7 (1997) C2-213.
- [19] A. Kuzmin, J. Purans, G. Dalba, P. Fornasini, F. Rocca, *J. Phys.: Condens. Matter* 8 (1996) 9083.
- [20] A. Kuzmin, J. Purans, *J. Phys.: Condens. Matter* 12 (2000) 1959.
- [21] J.J. Rehr, J. Mustre de Leon, S.I. Zabinsky, R.C. Albers, *J. Am. Chem. Soc.* 113 (1991) 5135.
- [22] J. Mustre de Leon, J.J. Rehr, S.I. Zabinsky, R.C. Albers, *Phys. Rev. B* 44 (1991) 4146.
- [23] A. Kuzmin, F. Rocca, to be published.
- [24] H. Ohtaki, T. Radnai, *Chem. Rev.* 93 (1993) 1157.
- [25] K.N.R. Taylor, M.I. Darby, *Physics of Rare-Earth Solids*, Chapman and Hall, London, 1972, p. 8.
- [26] Y. Zhou, Y.L. Lam, S.S. Wang, H.L. Liu, C.H. Kam, Y.C. Chan, *Appl. Phys. Lett.* 71 (1997) 587.
- [27] S. Todoroki, K. Hirao, N. Soga, *J. Appl. Phys.* 72 (1992) 5853.
- [28] Z. Wu, K. Lu, J. Dong, F. Li, Z. Fu, Z. Fang, *Z. Phys. B* 82 (1991) 15.